

# Elastic and Thermodynamic Properties of Anti-Perovskite Type Superconductor $\text{MCNi}_3$ ( $\text{M} = \text{Zn}, \text{Cd}$ )

M.Y. DUAN<sup>a</sup>, J.J. TAN<sup>a</sup>, G.F. JI<sup>b</sup>, X.-R. CHEN<sup>a,c,\*</sup> AND J. ZHU<sup>a</sup>

<sup>a</sup>College of Physical Science and Technology, Sichuan University, Chengdu 610064, China

<sup>b</sup>Laboratory for Shock Wave and Detonation Physics Research, Institute of Fluid Physics  
Chinese Academy of Engineering Physics, Mianyang 621900, China

<sup>c</sup>International Centre for Materials Physics, Chinese Academy of Sciences, Shenyang 110016, China

(Received March 6, 2010; in final form May 28, 2010)

The elastic and thermodynamic properties of the anti-perovskite superconductor  $\text{ZnCNi}_3$  and  $\text{CdCNi}_3$  are investigated by first-principles calculations. With the local density approximation as well as the generalized gradient approximation for exchange and correlation, the ground state properties and equation of state are obtained, which agree well with other theoretical calculations and experiments. Furthermore, by the elastic stability criteria, we predict that  $\text{ZnCNi}_3$  and  $\text{CdCNi}_3$  are not stable above 98.1 GPa and 196.5 GPa, respectively. The dependences of the heat capacity, thermal expansion coefficient, the Grüneisen parameter and bulk modulus ( $B_T$  and  $B_S$ ) on pressure and temperature for  $\text{ZnCNi}_3$  and  $\text{CdCNi}_3$  are also obtained successfully.

PACS numbers: 71.15.Mb, 62.20.D-, 91.60.Gf

## 1. Introduction

Soon after the discovery of 8 K intermetallic anti-perovskite superconductor compound  $\text{MgCNi}_3$  [1], the isostructural cubic anti-perovskites type  $\text{MCNi}_3$  ( $\text{M} = \text{Zn}, \text{Cd}$ ) have aroused great interest of scientists for their many puzzling physical properties. These compounds have the classical cubic perovskite structure with the oxygen atoms on the faces replaced by nickel atoms. All of them reside in the space group 221 ( $Pm\bar{3}m$ ). In the crystal of  $\text{MCNi}_3$ , the atoms occupy the positions:  $\text{M}(0; 0; 0)$ ,  $\text{C}(1/2; 1/2; 1/2)$  and  $\text{Ni}(0; 1/2; 1/2)$ . A carbon atom locates in the body-centered position surrounded by six nickel atoms to form an octahedral cage.

Up to now, most of experimental and theoretical investigations have been focused on superconductivity, density of states (DOS) and energy bands of  $\text{MCNi}_3$  [2–11]. Park et al. [3] found that the experimental data on  $\text{ZnCNi}_3$  shows that the Fermi level density of states is smaller than that of  $\text{MgCNi}_3$ , and argued that a strongly depressed DOS at the Fermi level could be responsible for pushing the transition temperature of  $\text{ZnCNi}_3$  below 2 K. Uehara et al. [8] observed that  $\text{CdCNi}_3$  is a superconductor with  $T_c = 2.5\text{--}3.2$  K. Moreover, the available experimental and theoretical data have shown that the physical properties of  $\text{MgCNi}_3$  material are very sensitive to external pressure, such as the superconducting transition temperature  $T_c$ , electronic and elastic properties [10, 11]. Therefore, a detailed study on the properties of  $\text{ZnCNi}_3$

and  $\text{CdCNi}_3$  under pressure and temperature is very necessary for their potential applications. The results may give useful insight toward proper understanding of the behaviors of  $\text{ZnCNi}_3$  and  $\text{CdCNi}_3$  superconductors.

In this work, we mainly focus on the mechanical stability and thermodynamic properties of  $\text{MCNi}_3$  under pressure and temperature by using the first-principles pseudopotential plane-wave method based on the density-functional theory and the quasi-harmonic Debye model [12]. The results obtained are in good agreement with the available experimental data and other theoretical results. In Sect. 2, we make a brief review of the theoretical methods. The results and some discussions are presented in Sect. 3. Finally, the conclusions are summarized in Sect. 4.

## 2. Theoretical calculations

### 2.1. Total energy electronic structure calculations

In the electronic structure calculations, the ultrasoft pseudopotentials introduced by Vanderbilt [13] are employed for all the ion–electron interactions, together with both the local density approximation (LDA) [14] and the generalized gradient approximation (GGA) [15] as exchange–correlation functions. A plane-wave basis set with an energy cut-off of 400 eV is applied. For the Brillouin zone sampling, we use an  $8 \times 8 \times 8$  Monkhorst–Pack mesh [16]. The self-consistent convergence of the total energy is  $10^{-6}$  eV/atom. Hydrostatic pressure, coupled with the variable cell approach, is applied within the Parrinello–Rahman method [17] to perform a full

\* corresponding author; e-mail: x.r.chen@tom.com

optimization of the cell structure for each target external pressure. All these total energy electronic structure calculations are implemented by using the CASTEP code [18].

## 2.2. Elastic properties

Elastic constants are defined by means of a Taylor expansion of the total energy,  $E(V, \delta)$ , for the system with respect to a small strain  $\delta$  of the lattice primitive cell volume  $V$ . The energy of a strained system is expressed as follows [19]:

$$E(V, \delta) = E(V_0, 0) + V_0 \left( \sum_i \tau_i \xi_i \delta_i + \frac{1}{2} \sum_{ij} C_{ij} \delta_i \xi_i \delta_j \right), \quad (1)$$

where  $E(V_0, 0)$  is the energy of the unstrained system with equilibrium volume  $V_0$ ,  $\tau_i$  is an element in the stress tensor, and  $\xi_i$  is a factor to take care of the Voigt index. It is known that for a cubic crystal structure there are only three independent of the elastic tensor components, i.e.  $C_{11}$ ,  $C_{12}$ ,  $C_{44}$ .

At the same time, the bulk modulus  $B$  and the shear modulus  $G$  are taken as

$$B = (C_{11} + 2C_{12})/3, \quad (2)$$

$$G = (3C_{44} + C_{11} - C_{12})/5. \quad (3)$$

Then the Young modulus  $E$  and the Poisson ratio  $\sigma$  is given by

$$E = \frac{9BG}{3B + G}, \quad (4)$$

$$\sigma = \frac{1}{2} (1 - E/3B). \quad (5)$$

The shear and longitudinal sound velocities  $V_s$  and  $V_l$  are obtained from Navier's equation as follows [20]:

$$V_s = \sqrt{\frac{G}{\rho}}, \quad V_l = \sqrt{\left( B + \frac{4}{3}G/\rho \right)}. \quad (6)$$

Furthermore, average wave velocity  $V_m$  is obtained from

$$V_m = \left[ \frac{1}{3} \left( \frac{2}{V_s^3} + \frac{1}{V_l^3} \right) \right]^{-1/3}. \quad (7)$$

Finally, with the average wave velocity  $V_m$ , the Debye temperature can be estimated [21]:

$$\Theta = \frac{\hbar}{k} \left[ \frac{3n}{4\pi} \left( \frac{N_A \rho}{M} \right) \right]^{1/3} V_m, \quad (8)$$

where  $\hbar$  is Planck's constant,  $k$  is Boltzmann's constant,  $N_A$  is Avogadro's number,  $n$  is the number of atoms per formula unit,  $M$  is the molecular mass per formula unit,  $\rho (= M/V)$  is the density.

## 2.3. Quasi-harmonic Debye model

To investigate the thermodynamic properties of  $\text{MCNi}_3$ , we here apply the quasi-harmonic Debye model [15], in which the phononic effect is considered. In the quasi-harmonic Debye model, the non-equilibrium Gibbs function  $G^*(V; P, T)$  takes the form of

$$G^*(V; P, T) = E(V) + PV + A_{\text{vib}}(\Theta(V); T), \quad (9)$$

where  $E(V)$  is the total energy per unit cell,  $PV$  corresponds to the constant hydrostatic pressure condition,  $\Theta(V)$  is the Debye temperature, and  $A_{\text{vib}}$  is the vibrational Helmholtz free energy that can be written as

$$A_{\text{vib}}(\Theta; T) = nkT \left[ \frac{9}{8} \frac{\Theta}{T} + 3 \ln(1 - e^{-\Theta/T}) - D(\Theta/T) \right], \quad (10)$$

where  $D(\Theta/T)$  represents the Debye integral,  $n$  is the number of atoms per formula unit. For an isotropic solid,  $\Theta$  is expressed by

$$\Theta = \frac{\hbar}{k} \left( 6\pi^2 V^{1/2} n \right)^{1/3} f(\sigma) \sqrt{\frac{B_S}{M}}, \quad (11)$$

where  $M$  is the molecular mass,  $B_S$  is the adiabatic bulk modulus and  $f(\sigma)$  are approximated by the static compressibility [22]

$$f(\sigma) = \left\{ 3 \left[ 2 \left( \frac{2}{3} \frac{1+\sigma}{1-2\sigma} \right)^{3/2} + \left( \frac{1}{3} \frac{1+\sigma}{1-\sigma} \right)^{3/2} \right]^{-1} \right\}^{1/3}, \quad (12)$$

$$B_S \cong B(V) = V \left\{ \frac{d^2 E(V)}{dV^2} \right\}. \quad (13)$$

The Poisson  $\sigma$  is obtained from Eq. (5). Therefore, the non-equilibrium Gibbs function  $G^*(V; P, T)$  can be minimized with respect to volume  $V$ :

$$\left( \frac{\partial G^*(V; P, T)}{\partial V} \right)_{P, T} = 0, \quad (14)$$

and one could obtain the thermal equation of state and the thermal expansion coefficient  $\alpha$  as follows:

$$\alpha = \gamma C_V / (B_T V), \quad (15)$$

where the isothermal bulk modulus  $B_T$ , the heat capacity  $C_V$  and the Grüneisen parameter  $\gamma$  are expressed as

$$B_T(P, T) = V \left[ \frac{\partial^2 G^*(V; P, T)}{\partial V^2} \right]_{P, T}, \quad (16)$$

$$C_V = 3nk \left[ 4D(\Theta/T) - \frac{3\Theta/T}{e^{\Theta/T} - 1} \right], \quad (17)$$

$$\gamma = - \frac{d \ln \Theta(V)}{d \ln V}. \quad (18)$$

## 3. Results and discussion

### 3.1. Structure and equation of state

At first, a series of lattice constants  $a$  are set to obtain the total energy  $E$  and the corresponding primitive cell volume  $V$  through both GGA and LDA schemes. By fitting the  $E$ - $V$  data to the numerical equation of state (EOS) [12], we can obtain the equilibrium lattice constant  $a_0$ , bulk modulus  $B_0$  and its pressure derivation  $B'_0$  at  $P = 0$  GPa and  $T = 0$  K, which are listed in Table I, together with the available experimental and other theoretical data [3–9, 23, 24].

TABLE I

Lattice constants ( $\text{\AA}$ ), bulk modulus  $B_0$  (GPa) and its pressure derivative  $B'_0$  of  $\text{MCNi}_3$  at 0 GPa and 0 K.

MCNi <sub>3</sub>	Parameters	Present work		Other work		Experiments
		GGA	LDA	GGA	LDA	
ZnCNi <sub>3</sub>	$a_0$	3.7856	3.6985	3.78 <sup>a</sup> , 3.8236 <sup>b</sup>	3.69 <sup>a</sup> , 3.679 <sup>c</sup> , 3.7338 <sup>b</sup>	3.66 <sup>f</sup> , 3.77 <sup>g</sup>
	$B_0$	197.46	243.3	176.99 <sup>d</sup>		251 <sup>c</sup>
	$B'_0$	4.67	4.50			
CdCNi <sub>3</sub>	$a_0$	3.8830	3.7913	3.871 <sup>e</sup> , 3.867 <sup>d</sup> , 3.8668 <sup>i</sup>	3.777 <sup>e</sup>	3.844 ± 0.001 <sup>h</sup>
	$B_0$	182.47	227.35	152.77 <sup>d</sup> , 188.31 <sup>i</sup> , 182.65 <sup>e</sup>	228.39 <sup>e</sup>	
	$B'_0$	4.80	4.67	4.77 <sup>e</sup>	4.76 <sup>e</sup>	

<sup>a</sup> Ref. [4]; <sup>b</sup> Ref. [5]; <sup>c</sup> Ref. [6]; <sup>d</sup> Ref. [9]; <sup>e</sup> Ref. [7]; <sup>f</sup> Ref. [3]; <sup>g</sup> Ref. [23]; <sup>h</sup> Ref. [8]; <sup>i</sup> Ref. [24]

For ZnCNi<sub>3</sub>, our lattice constant  $a_0$  from GGA and LDA approaches are close to those given by Sieberer et al. and Joseph et al. [4, 5]. Their experimental data have the difference of 0.11  $\text{\AA}$ . Our LDA result approaches the former [3] and GGA result seems to approach the latter [23]. Exceptionally, Park et al. experimental value (3.66  $\text{\AA}$ ) is smaller than all theoretical LDA results [4–6] and other experimental results [23]. This directly leads to the Johannes and Pickett further research. They suggested a larger lattice constant (probably near 3.74  $\text{\AA}$ ) than their theoretical data (3.679  $\text{\AA}$ ) [6] for stoichiometric ZnCNi<sub>3</sub>. The suggested lattice constant is perfect between our GGA and LDA results, just like the same cases for isostructural MgCNi<sub>3</sub> [11] and CdCNi<sub>3</sub> whose theoretical data are compared with experimental data [8]. For CdCNi<sub>3</sub>, our results are consistent with the Uehara et al. experimental results [8], the present  $B_0$  and  $B'_0$  are very close to the Wu et al. [7] while have some difference with the Shein et al. calculations [9]. It is easily found that almost all the theoretical calculations for the lattice constants by GGA are overestimated, and those by LDA are underestimated. The atomic radii ( $M = \text{Zn, Cd}$ ) are 1.39  $\text{\AA}$  and 1.56  $\text{\AA}$  respectively, and  $a_0$  (ZnCNi<sub>3</sub>) <  $a_0$  (CdCNi<sub>3</sub>) is reasonable.

In addition, the normalized volume  $V/V_0$  calculated as a function of pressure for MCNi<sub>3</sub> is plotted in Fig. 1. The relative volume decreases almost linearly with the pressure increases. When the applied pressure equals to 100 GPa, the cell volume for ZnCNi<sub>3</sub> and CdCNi<sub>3</sub>, respectively, become 76.2% and 75.8% of the zero pressure equilibrium cell volume. It is clearly seen that ZnCNi<sub>3</sub> is compressed more difficult than CdCNi<sub>3</sub>.

### 3.2. Elastic constants and mechanical stability

The elastic constants of solids provide a link between the mechanical and dynamical behaviors of crystals, and give important information concerning the nature of the forces operating in solids. The Debye temperature  $\Theta_D$  correlates with many physical properties of solids, such as specific heat, phonon frequency, thermal coefficient and melting temperature.

In Table II, the elastic constants  $C_{11}$ ,  $C_{12}$ ,  $C_{44}$ , longitudinal, shear and average wave velocities  $V_l$ ,  $V_s$ ,  $V_m$  and

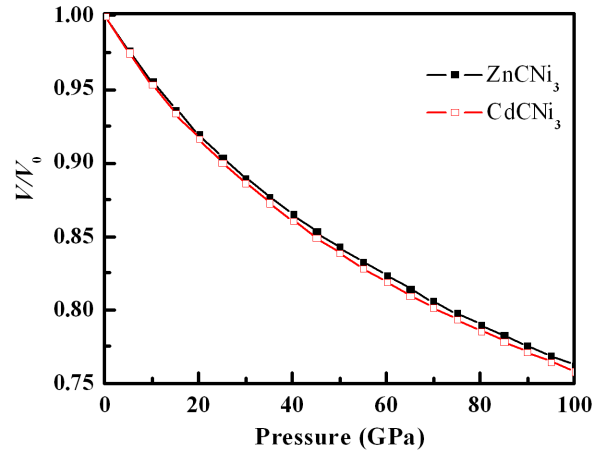


Fig. 1. Changes of the relative volume of MCNi<sub>3</sub> with increasing pressure.

Debye temperature  $\Theta_D$  of MCNi<sub>3</sub> at  $P = 0$  and  $T = 0$  are listed. The  $V_l$ ,  $V_s$ ,  $V_m$  and  $\Theta_D$  are calculated with the obtained elastic constants from Eq. (6), Eq. (7) and Eq. (8). Due to an underestimate of the lattice constant, the elastic constants calculated by LDA are larger than those by GGA. Though there are no experimental wave velocities for comparison, our results are very close to the experimental wave velocities of the isostructural MgCNi<sub>3</sub>, and are smaller than other theoretical calculations [7, 25]. For ZnCNi<sub>3</sub>, the Debye temperature  $\Theta_D$  is very close to the Park et al. experimental data by analyzing X-ray diffraction (XRD) data [3]. For CdCNi<sub>3</sub>, though the obtained  $\Theta_D$  is larger than that of the Uehara et al. experimental data, the obtained sequence of  $\Theta_D$  by GGA:  $\Theta_D$  (ZnCNi<sub>3</sub> = 424) >  $\Theta_D$  (CdCNi<sub>3</sub> = 405) >  $\Theta_D$  (MgCNi<sub>3</sub> = 283) are consistent with the experimental sequence:  $\Theta_D$  (ZnCNi<sub>3</sub> = 421) >  $\Theta_D$  (CdCNi<sub>3</sub> = 352) >  $\Theta_D$  (MgCNi<sub>3</sub> = 287) [3, 8, 11, 26]. Correspondingly a decrease of the Debye temperature, the averaged phonon frequency should also decrease among the three anti-perovskite superconductors.

TABLE II

Calculated elastic constants in GPa, longitudinal, shear and average wave velocity ( $V_l$ ,  $V_s$  and  $V_m$ ) in  $\text{m s}^{-1}$  and the Debye temperature  $\Theta_D$  in K at 0 GPa and 0 K.

		Methods	$C_{11}$	$C_{12}$	$C_{44}$	$V_l$	$V_m$	$V_s$	$\Theta_D$
ZnCNi <sub>3</sub>	Present	GGA	349.94	121.23	38.88	5992	3154	2802	424
		LDA	427.45	143.02	41.73	6325	33273	2905	450
	Other cal.	GGA	319.53 <sup>a</sup>	105.72 <sup>a</sup>	39.42 <sup>a</sup>				
		MRIM	344 <sup>b</sup>	110 <sup>b</sup>	64 <sup>b</sup>	6858 <sup>b</sup>	4024 <sup>b</sup>	3598 <sup>b</sup>	302 <sup>b</sup>
	Exp. [3]								421
CdCNi <sub>3</sub>	Present	GGA	302.17	124.82	52.34	5629	3094	2755	405
		LDA	380.60	156.45	58.80	6046	3246	2887	435
	Other cal.	GGA	337.26 <sup>c</sup>	105.34 <sup>c</sup>	57.36 <sup>c</sup>	6159 <sup>c</sup>	3536 <sup>c</sup>	3156 <sup>c</sup>	
			255.0 <sup>a</sup>	101.65 <sup>a</sup>	58.39 <sup>a</sup>				
		LDA	423.80 <sup>c</sup>	130.69 <sup>c</sup>	67.12 <sup>c</sup>	5750 <sup>c</sup>	3334 <sup>c</sup>	2979 <sup>c</sup>	
	Exp. [8]	MRIM	341 <sup>b</sup>	127 <sup>b</sup>	72 <sup>b</sup>	7014 <sup>b</sup>	4087 <sup>b</sup>	3653 <sup>b</sup>	307 <sup>b</sup>
								352	

<sup>a</sup> Ref. [9]; <sup>b</sup> Ref. [25]; <sup>c</sup> Ref. [7]

Pettifor [27] suggested that the angular character of atomic bonding in metals and compounds could be described by the Cauchy pressure  $C_{12}-C_{44}$ . If the bonding in character is metallic, the Cauchy pressure is typically positive. If the bonding in character is directional and with a lower mobility, the Cauchy pressure is typically negative. The rule has been used in the study of ductile materials (Ni, Al), brittle semiconductors (Si) and alloying effects on TiN-based nitrides [27, 28]. The values of the calculated Cauchy pressures  $C_{12}-C_{44}$  of ZnCNi<sub>3</sub> and CdCNi<sub>3</sub> are 82.35 GPa and 72.48 GPa at zero pressure, respectively. Due to the typically positive values of the Cauchy pressure, the MCNi<sub>3</sub> should belong to metallic bonding materials.

Recently, the elastic constants and mechanical stabilities of crystals have attracted much interest by physicists [29]. In 2002, Sin'ko and Smirnov [29] deduced the conditions of mechanical stability from elastic constants. As is known, for a cubic crystal, the mechanical stability under isotropic pressure is judged from the following condition:

$$\tilde{C}_{44} > 0, \quad \tilde{C}_{11} > |\tilde{C}_{12}|, \quad \tilde{C}_{11} + 2\tilde{C}_{12} > 0, \quad (19)$$

where  $\tilde{C}_{\alpha\alpha} = C_{\alpha\alpha} - p$  ( $\alpha = 1, 4$ ),  $\tilde{C}_{12} = C_{12} + p$ . The elastic constants of MCNi<sub>3</sub> under pressure obtained are illustrated in Fig. 2. It is seen that  $C_{11}$ ,  $C_{12}$  and  $C_{44}$  increase with the enhancement of pressure. The change of  $C_{11}$  is more sensitive to pressure than other two, while  $C_{44}$  is the most unresponsive one.

Figure 3 presents the  $\tilde{C}_{44}$  versus pressure for MCNi<sub>3</sub>. By fitting  $\tilde{C}_{44}$  data to second-order polynomials, we find that the pressures of ZnCNi<sub>3</sub> and CdCNi<sub>3</sub> are above 98.1 GPa and 196.5 GPa, respectively,  $\tilde{C}_{44} > 0$  is no longer fulfilled, which indicated that ZnCNi<sub>3</sub> and CdCNi<sub>3</sub>

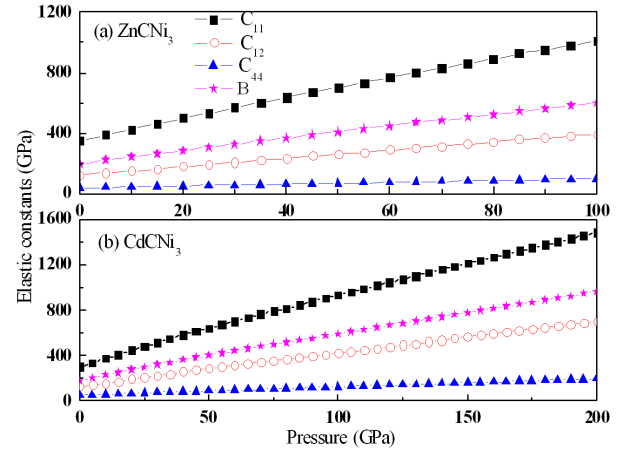


Fig. 2. The dependence of  $C_{ij}$  and  $B$  of MCNi<sub>3</sub> on pressure.

are not mechanically stable at above the pressures. In our former work, the obtained critical pressure of MgCNi<sub>3</sub> is 58.4 GPa [11], which is reasonable by comparing some experimental data. In fact, according to our experience, the phase transition pressure should be smaller than the critical mechanical stable pressure.

### 3.3. Thermodynamic properties

The quasi-harmonic Debye model empowers us to obtain heat capacity  $C_V$ , thermal expansion coefficient  $\alpha$ , Grüneisen parameter  $\gamma$  and bulk modulus on temperature and pressure. In Fig. 4, we plot the dependence of heat capacity  $C_V$  on temperature at 0 and 95 GPa, respectively. It is readily seen that when  $T < 500$  K,

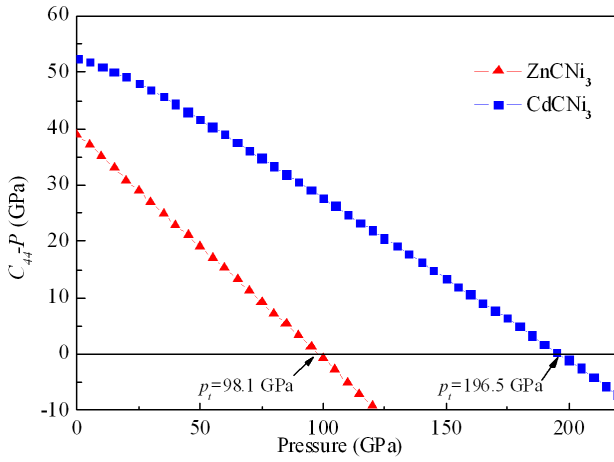


Fig. 3. The mechanical stability of  $\text{MCNi}_3$  versus pressure at 0 K.

the  $C_V$  of  $\text{MCNi}_3$  are strongly dependent on the temperature and pressure. This is due to the anharmonic approximations of the Debye model used here. At higher pressures and higher temperatures, the anharmonic effect on  $C_V$  is suppressed, and  $C_V$  is close to a constant. The calculated  $C_V$  of  $\text{CdCNi}_3$  is slightly larger than  $C_V$  of  $\text{ZnCNi}_3$ . However, our results are significantly smaller than the Kaur et al. theoretical calculation results for both  $\text{ZnCNi}_3$  and  $\text{CdCNi}_3$  until  $T > 600$  K [25].

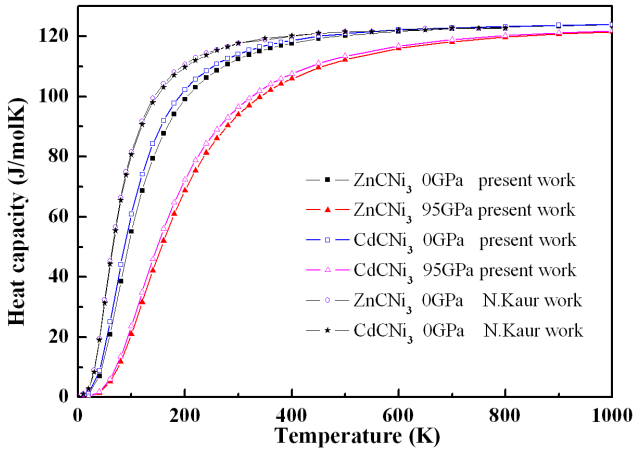


Fig. 4. Temperature dependences of heat capacity for  $\text{MCNi}_3$  at 0 and 95 GPa, compared with the previous calculation [25].

In Fig. 5, we present the variations of the thermal expansion coefficient  $\alpha$  with temperature and pressure. At a given temperature, the thermal expansion coefficient  $\alpha$  of  $\text{ZnCNi}_3$  and  $\text{CdCNi}_3$  decrease rapidly as the pressure enhances. However, the  $\alpha$  increases exponentially with  $T$  at low temperatures and gradually approaches a linear increase at high temperatures. It is noted that the curves of 300 K and 1000 K seem to be parallel to each other, and the  $\alpha$  of  $\text{ZnCNi}_3$  and  $\text{CdCNi}_3$  are almost exactly the

same at 300 K. At the room temperature and zero pressure, the  $\alpha$  of  $\text{ZnCNi}_3$  and  $\text{CdCNi}_3$  are  $4.08 \times 10^{-5} \text{ K}^{-1}$  and  $4.14 \times 10^{-5} \text{ K}^{-1}$ , respectively.

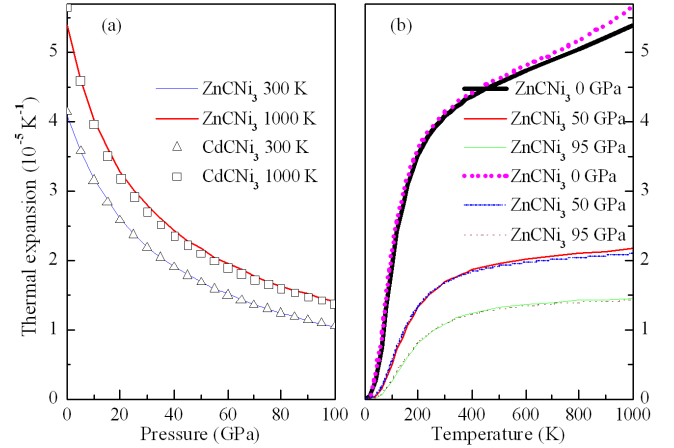


Fig. 5. Thermal expansion coefficient  $\alpha$  versus pressure and temperature for  $\text{MCNi}_3$ .

The Grüneisen parameter  $\gamma$  could describe the alteration in vibration of a crystal lattice based on the increase or decrease in volume as a result of temperature change. Recently, it has been widely used to characterize and extrapolate the thermodynamic properties of materials at high pressures and high temperatures. In Fig. 6, the variations of the Grüneisen parameter  $\gamma$  with pressure and temperature are displayed, from which it can be found that the Grüneisen parameter  $\gamma$  increases with increasing temperature at a given pressure and decreases with increasing pressure at a given temperature. These results are due to the fact that the effect of increasing pressure on the material is the same as that of decreasing temperature on it. At zero pressure the Grüneisen parameter  $\gamma$  obviously increases with temperature, but the increasing tendency become more weak after  $P = 50$  and 95 GPa for  $\text{ZnCNi}_3$  and  $\text{CdCNi}_3$ , respectively.

The dependences of isothermal ( $B_T$ ) and adiabatic ( $B_S$ ) bulk modulus of  $\text{MCNi}_3$  on temperature at zero pressure are illustrated in Fig. 7. It can be found that  $B_T$  and  $B_S$  are nearly constant from 0 K to 100 K and then decrease almost linearly with increasing temperatures, as is obvious from the relationship  $B_S = B_T(1 + \alpha\gamma T)$ .  $B_T$  and  $B_S$  coincide at low temperature and then diverge with rising  $T$ . At room temperature,  $\text{d}B_T/\text{d}T$  of  $\text{ZnCNi}_3$  and  $\text{CdCNi}_3$  are  $-0.0392$  and  $-0.0403$  GPa/K and  $\text{d}B_S/\text{d}T$  are  $-0.0181$  and  $-0.0208$  GPa/K, respectively. The variety of  $\text{d}B_T/\text{d}T$  is much stronger than that of  $\text{d}B_S/\text{d}T$ .

#### 4. Conclusions

The elastic and thermodynamic properties of the anti-perovskite superconductor  $\text{MCNi}_3$  under pressure are

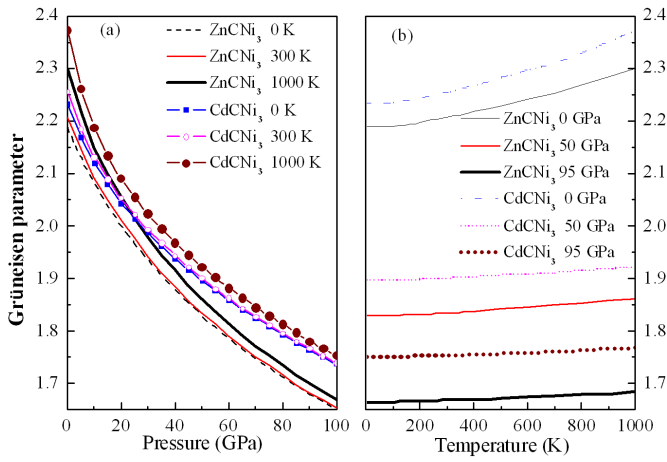


Fig. 6. Pressure (a) and temperature (b) dependences of Grüneisen parameter  $\gamma$  for MCNi<sub>3</sub>.

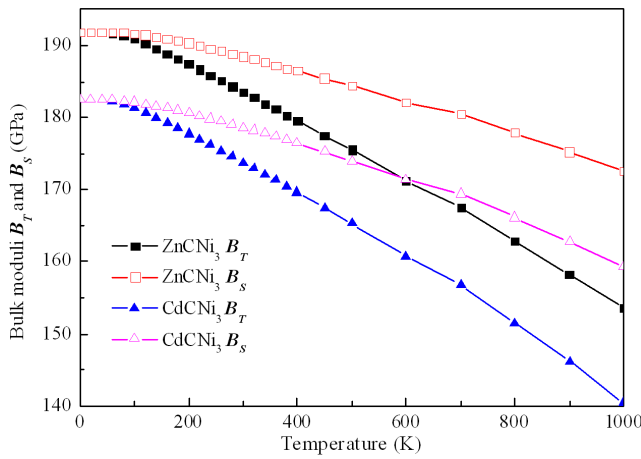


Fig. 7. Temperature dependence of isothermal ( $B_T$ ) and adiabatic ( $B_S$ ) zero-pressure bulk modulus for MCNi<sub>3</sub>.

investigated by first-principles calculations with the local density approximation as well as the generalized gradient approximation for exchange and correlation. The ground state properties and equation of state of MCNi<sub>3</sub> are obtained, which agree well with both theoretical calculations and experiments. We conclude that MCNi<sub>3</sub> should belong to metallic bonding materials by analyzing their elastic modulus. From the high pressure elastic constants, we predict that ZnCNi<sub>3</sub> and CdCNi<sub>3</sub> are not stable above 98.1 GPa and 196.5 GPa, respectively. Lastly, some thermodynamic properties such as the heat capacity, thermal expansion coefficient, the Grüneisen parameter and bulk modulus ( $B_T$  and  $B_S$ ) under different pressures and temperatures are also successfully obtained. Our calculations show that the ZnCNi<sub>3</sub> and CdCNi<sub>3</sub> are very similar in structural, elastic and thermodynamic properties.

## Acknowledgments

The authors would like to thank the support by the National Natural Science Foundation of China under grant No. 10776022 and by the Specialized Research Fund for the Doctoral Program of Higher Education under grant No. 20090181110080. We also acknowledge the support for the computational resources by the State Key Laboratory of Polymer Materials Engineering of China in Sichuan University.

## References

- [1] T. He, Q. Huang, A.P. Ramirez, Y. Wang, K.A. Regan, N. Rogado, M.A. Hayward, M.K. Haas, J.S. Slusky, K. Inumara, H.W. Zandbergen, N.P. Ong, R.J. Cava, *Nature* **411**, 54 (2001).
- [2] S. Bağcı, S. Duman, H.M. Tütüncü, G.P. Srivastava, *Phys. Rev. B* **78**, 174504 (2008).
- [3] M.S. Park, J.S. Giim, S.H. Park, Y.W. Lee, S.I. Lee, E.J. Choi, *Supercond. Sci. Technol* **17**, 274 (2004).
- [4] M. Sieberer, P. Mohn, J. Redinger, *Phys. Rev. B* **75**, 024431 (2007).
- [5] P. Joseph, P.P. Singh, *J. Phys., Condens. Matter* **18**, 5333 (2006).
- [6] M.D. Johannes, W.E. Pickett, *Phys. Rev. B* **70**, 060507 (2004).
- [7] S.Q. Wu, Z.F. Hou, Z.Z. Zhu, *Solid State Sci.* **11**, 251 (2009).
- [8] M. Uehara, T. Yamazaki, T. Kori, T. Kashida, Y. Kimishima, I. Hase, *J. Phys. Soc. Jpn.* **76**, 034714 (2007).
- [9] I.R. Shein, V.V. Bannikov, A.L. Ivanovskii, *Physica C* **468**, 1 (2008).
- [10] G. Garbarino, M. Monteverde, M. Nñez-Regueiro, C. Acha, R. Weht, T. He, K.A. Regan, N. Rogado, M. Hayward, R.J. Cava, *Physica C* **408**, 754 (2004).
- [11] W. Zhang, X.R. Chen, L.C. Cai, F.Q. Jing, *J. Phys., Condens. Matter* **20**, 325228 (2008).
- [12] M.A. Blanco, E. Francisco, V. Luana, *Comput. Phys. Commun.* **158**, 57 (2004).
- [13] D. Vanderbilt, *Phys. Rev. B* **41**, 7892 (1990).
- [14] S.H. Vosko, L. Wilk, M. Nusair, *Can. J. Phys.* **58**, 1200 (1980).
- [15] J.P. Perdew, K. Burke, M. Ernzerhof, *Phys. Rev. Lett.* **77**, 3865 (1996).
- [16] H.J. Monkhorst, J.D. Pack, *Phys. Rev. B* **13**, 5188 (1976).
- [17] M. Parrinello, A. Rahman, *Phys. Rev. Lett.* **45**, 1196 (1980).
- [18] V. Milman, B. Winkler, J.A. White, C.J. Packard, M.C. Payne, E.V. Akhmatkaya, R.H. Nobes, *Int. J. Quant. Chem.* **77**, 895 (2000).
- [19] L. Fast, J.M. Wills, B. Johansson, O. Eriksson, *Phys. Rev. B* **51**, 17431 (1995).
- [20] E. Schreiber, O.L. Anderson, N. Soga, *Elastic Constants and Their Measurements*, McGraw-Hill, New York 1973.
- [21] O.L. Anderson, *J. Phys. Chem. Solids* **24**, 909 (1963).

- [22] E. Francisco, J.M. Recio, M.A. Blanco, A. Martín-Pendás, A. Costales, *J. Phys. Chem.* **102**, 1595 (1998).
- [23] J.B. Goodenough, M. Longo, in: *Magnetic and Other Properties of Oxides and Related Compounds*, Eds. K.-H. Hellwege, A.M. Hellwege, Landolt-Börnstein-Group III Condensed Matter, New Series, Vol. 4, Part A Springer-Verlag, Berlin 1970, p. 266.
- [24] I.R. Shein, A.L. Ivanovskii, *Phys. Rev. B* **77**, 104101 (2008).
- [25] N. Kaur, R. Mohan, N.K. Gaur, R.K. Singh, *J. Alloys Comp.* **491**, 284 (2010).
- [26] I.N. Frantsevich, F.F. Voronov, S.A. Bokuta, in: *Elastic Constants and Elastic Moduli of Metals and Insulators Handbook*, Ed. I.N. Frantsevich, Naukova Dumka, Kiev 1983, p. 60.
- [27] D.G. Pettifor, *Mater. Sci. Technol.* **8**, 345 (1992).
- [28] K. Chen, L.R. Zhao, J. Rodgers, J.S. Tse, *J. Phys. D, Appl. Phys.* **36**, 2725 (2003).
- [29] G.V. Sin'ko, N.A. Smirnov, *J. Phys., Condens. Matter* **14**, 6989 (2002).